Seiffert, S.; Friess, F.; Lendlein, A.; Wischke, C.:

Faster Droplet Production by Delayed Surfactant-Addition in Two-Phase Microfluidics to form Thermo-Sensitive Microgels

In: Journal of Colloid and Interface Science (2015) Elsevier

DOI: /10.1016/j.jcis.2015.04.017

Faster Droplet Production by Delayed Surfactant-Addition in Two-Phase Microfluidics to form Thermo-Sensitive Microgels

Sebastian Seiffert [a,b,c,+,*], Fabian Friess [a,d,+], Andreas Lendlein [a,b,d], Christian Wischke [a,d,*]

[a] Helmholtz Virtual Institute „Multifunctional Biomaterials for Medicine“, Kantstr. 55, D-14513 Teltow, Germany.

[b] Institute of Chemistry and Biochemistry, Freie Universität Berlin, Takustr. 3, D-14195 Berlin, Germany.

[c] Soft Matter and Functional Materials, Helmholtz-Zentrum Berlin, Hahn-Meitner-Platz 1, D-14109 Berlin, Germany

[d] Institute of Biomaterial Science and Berlin-Brandenburg Center for Regenerative Therapies, Helmholtz-Zentrum Geesthacht, Kantstr. 55, D-14513 Teltow, Germany.

+ These authors contributed equally to this work.

* Corresponding authors. Fax: +49 (0)3328 352 452 E-mail addresses: christian.wischke@hzg.de (C. Wischke), seiffert@chemie.fu-berlin.de (S. Seiffert)

Abstract

Microfluidic droplet templating produces monodisperse particles of well controllable sizes, but this is limited by the necessity to operate microfluidic devices at low flow rates in the dripping regime. Here, the per-channel rate of droplet production could be substantially increased by delayed surfactant addition as applied and verified for microfluidic production of *N*-isopropylacrylamide based microgels.

Keywords: Droplet based microfluidics, rapid production, microgel

1. Introduction

Microgels are micrometer-scale particles that consist of a crosslinked polymer network swollen by solvent, typically water [1,2]. Microgels can be designed to be sensitive to changes in their environment, for example, to changes in temperature, allowing them to be selectively swollen and deswollen in response to external stimulation [3,4]. Such responsivity relies on delicate hydrogen-bonding and hydrophobic interactions between the polymer and the solvent, which is achieved by the use of polymers that consist of amphiphilic monomer repeat units, the most prominent of which being poly(*N*-isopropylacrylamide) [4]. The original use of the term microgel referred to particles with sub-micrometer-scale colloidal dimensions, down to single, intramolecular crosslinked polymer coils [1], whereas recent contributions have extended its use to larger, above-micrometer-scale particles [5]. The prime utility of such above-colloidal microgels is their ability to encapsulate additives with above-

molecular and above-colloidal sizes within a local environment similar to natural tissue [3,6]. As a result, these microgels are promising for applications in the biomedical field [7], especially when they exhibit environmental sensitivity to physiologically relevant changes of temperature or pH.

To optimize the utility of such above-colloidal-scale microgels, it is necessary to control their size and shape in addition to controlling their chemical function. This challenge can be addressed by droplet-based microfluidic templating [8,9]. In this approach, a stream of an aqueous pre-microgel solution (dispersed phase) is created in a microchannel and then periodically broken to form droplets by flow focusing with an immiscible oil (continuous phase). The size of the resulting pre-microgel droplets is controlled by the fluid flow rates, the dimension of the microchannel, and the fluid interfacial tension [10].

Despite its great promise, an intrinsic limitation in the use of droplet-based microfluidics for templating monodisperse microgels is the necessity to operate at low flow rates to avoid the transition from dripping to jetting regime [10]. When both the inner dispersed and the outer continuous phase are injected into a microfluidic device at low rates, individual monodisperse drops of the inner fluid within the outer fluid are formed periodically in a process termed dripping. By contrast, if the flow rate of either of these fluids is increased beyond a certain limit, this results in a jet of the inner fluid with drops forming far further downstream with, typically, a broader size distribution. The onset of the dripping-to-jetting transition is assessed by the capillary number $Ca = \eta \cdot \dot{v} \cdot \sigma^{-1}$ (Eq. 1) of the outer fluid and the Weber number $We = \rho \cdot \dot{v}^2 \cdot d \cdot \sigma^{-1}$ (Eq. 2) of the inner fluid.

In these equations, η is the viscosity, $\dot{v}$ the flow speed, and ρ the density of the respective fluid, along with d the channel diameter and σ the interfacial tension between the two immiscible phases. The Ca of the outer fluid reflects the balance between the drag of the outer fluid pulling on the inner fluid and interfacial tension that resists the flow in the jet as droplet pinch-off occurs. The We of the inner fluid reflects the balance between inertial forces of the inner liquid pushing the drop downstream and, again, interfacial tension resisting the flow. The boundary between dripping and jetting has previously been detected when either number, or their sum, is roughly in the range of unity, considering possible deviations up to one order of magnitude [10].

Thus, controlled microfluidic fabrication of particles must occur at low flow rates to keep both of the above numbers small. To overcome the resulting limitation of productivity that impairs the utility of microfluidic templates in industrial-scale processes, a parallelization of microfluidic channels being operated simultaneously or a droplet splitting has been suggested

[11,12,13]. In addition to this approach, however, it would be desirable to increase the productivity of each individual microfluidic channel, too. This task must tackle the challenge of operating in the controlled dripping regime at higher flow rates. Here, we present a way to increase the per-channel rate in the production of water-based microgels in droplet-based microfluids by delayed surfactant addition.

2. Experimental

The used chemicals were fluorocarbon oil HFE-7500 (3M), fluorinated surfactant Krytox 157 FSL (DuPont), *N*,*N*,*N*',*N*'-tetramethylethylenediamine (TEMED), *N*-isopropylacrylamide (NIPAAm), *N*,*N*'-methylene bisacrylamide (BIS) and ammonium persulfate (APS) (all latter by Sigma-Aldrich).

Microfluidic devices with a double cross-junction geometry (see Fig. 1 and 2) were fabricated through soft lithography in PDMS by bonding a PDMS replica of a pre-designed array of channels onto a glass slide using oxygen plasma treatment [14]. After the plasma treatment, the channels were coated by injecting a water repellent mixture of fluorinated compounds (Aquapel; PPG Industries, Pittsburgh, PA, USA) into the channels to render them hydrophobic and optimize their wettability for the formation of water-in-oil emulsions [15]. To operate the devices, three fluids were supplied by three syringe pumps (AL 1010, WPI, Sarasota, FL, USA) at given equal volume flow rates (q, see Fig. 2A-D) through polyethylene tubing (ID = 0.38 mm, OD = 1.09 mm, Becton Dickinson, Sparks, MD, USA).

Droplet formation was monitored by a digital high-speed microscope (VW 6000E with VH-Z100R lens and VW 100C camera, Keyence Deutschland GmbH, Neu-Isenburg, Germany). Images of the finally collected droplets were obtained on an optical microscope (DMI6000B, Leica, Wetzlar, Germany) and sizes were analyzed (more than 300 drops, each) after contrast adjustment and applying a watershed filter using ImageJ software (National Institutes of Health, USA). The droplet-number formation frequencies, $f = q \cdot V_{\mathrm{drop}}^{-1}$, were calculated from the volumetric throughput of the dispersed phase in the microfluidic experiments, q, and the droplet volumes (V_{drop}), which were calculated from the droplet average diameters. A tensiometer (K 100, Kruess GmbH, Hamburg, Germany) was operated at 25 °C with a density measurement setup (DE0701, silicon standard probe with 2.33 $\mathrm{g \cdot cm^{-3}}$, Kruess GmbH, Germany) to determine the densities (ρ) of the different fluids used in this work; it was also operated with a Wilhelmy-plate (PL01, platinum, $19.9 \times 0.2 \times 10.0\ \mathrm{mm^3}$, Kruess GmbH, Germany) to estimate the interfacial tensions (σ) of the different pairs of fluids, respectively. Kinematic viscosities (v) were determined at 25 °C using an Ubbelohde viscometer with

Hagenbach correction (PVS1, S5 test stand, E200 thermostat, Koenigshofen, Germany). Dynamic viscosities (η) were calculated by $\eta = \nu \cdot \rho$.

3. Results and Discussion

The conventional approach for microfluidic droplet formation in two-phase systems involves controlled dispersion of an inner fluid in a stabilizer-doped continuous phase with a microfluidic device operating in the controlled dripping regime, as shown in Fig. 1A. This may potentially be followed by addition of a further fraction of continuous phase that contains additives such as accelerators to induce downstream droplet-gelation [15], as shown in Fig. 1B. The limitation of this method is that increased Capillary (*Ca*) and Weber (*We*) numbers by increased volumetric flows will result in uncontrolled jetting, as shown in the inset of Fig. 1B. The approach presented in this paper aims to overcome this limitation and to increase the rate of droplet formation by decreasing *Ca* and *We* of the outer and inner fluids, which is achieved by increasing their interfacial tension (σ). With this strategy, microfluidic devices with a given channel size (d) can be operated at higher flow rates (q) before the undesired dripping-to-jetting transition occurs. To achieve this, an external phase without any surfactant is used, as illustrated in Fig. 1C. This mode of operation assures maximally possible interfacial tension with the inner pre-microgel phase. To prevent the pre-microgel droplets from coalescing, surfactant is added directly after their formation in the microfluidic channel, as also illustrated in Fig. 1C. With this approach, the droplet formation can be separated from the droplet stabilization, allowing the first to occur at maximal rate while still ensuring the second.

As a model material, poly(*N*-isopropylacrylamide) (pNIPAAm) is chosen because of its relevance for producing gels and microgels with a tunable volume-phase transition temperature close to the human body temperature [4, 16]. This materials, however, poses a severe challenge in view of microfluidic dispersion of aqueous solutions of its monomer, *N*-isopropylacrylamide (NIPAAm), in a continuous oil phase. As an amphiphilic molecule, *N*-isopropylacrylamide has a strong interfacial activity. Whereas this is beneficial in view of gaining a thermo-responsive polymer gel [4, 16], it is disadvantageous during the microfluidic particle templating, because it lowers the interfacial tension between the monomer fluid and the external oil and thus requires microfluidic production at low flows rates according to Eq. (1) and (2). Since the low interfacial activity of the NIPAAm-based monomer fluid is not sufficient to prevent coalescence of emulsion droplets, further addition of surfactant to the

external phase is required. In the conventional microfluidic set-up, this lowers the maximal flow rates that ensures a controlled dripping regime even more.

The outer fluid in the present study was the fluorocarbon carbon oil HFE-7500 along with fluorinated surfactant Krytox 157 FSL (3.6 vol.%, applied in a single channel or 1.8 vol.%, applied in both channels), which is a widely employed oil in biomicrofluidics [17].

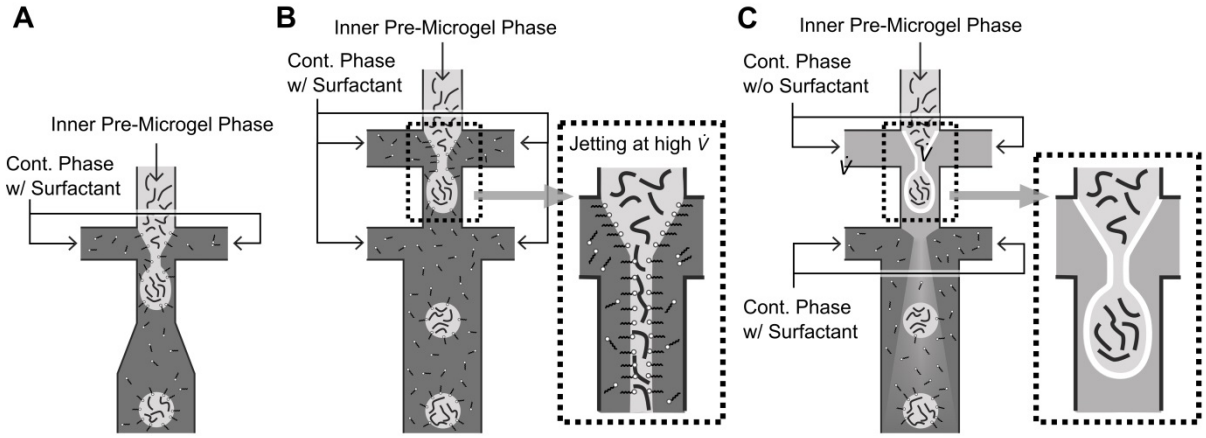

Fig. 1: Schemes of microfluidic droplet formation for microgel-particle templating. (A, B) Conventional approaches of droplet formation in two-phase microfluidics, either using a single cross-junction (A) or a double-cross-junction geometry (B), the latter allowing additional components such as initiators for droplet gelation [15] to be separately added to the continuous phase. The limitation of both of these modes of operation is that increased flow rates will result in uncontrolled jet formation, as illustrated in the inset-zoom. (C) This work's concept to overcome this limitation and to enhance the rate of droplet production is based on separating the processes of droplet formation and droplet stabilization in a microfluidic device with two sequential cross-junction channels. In the first cross-junction, droplets are formed in the controlled dripping regime at high rate without surfactant being present. In the second cross-junction, surfactant is added to the continuous phase to prevent downstream droplet coalescence.

Table 1: Viscosities and densities of the fluids used in this work, measured at 25 °C.

Fluid	Kin. Viscosity[1] (ν, $mm^2 \cdot s^{-1}$)	Density[2] (ρ, $g \cdot mL^{-1}$)	Dyn. Viscosity (η, mPa·s)
Water	0.908	0.996	0.904
Monomer solution [3]	1.29	1.399	1.80
HFE-7500	0.771	1.62	1.25
HFE-7500 w/surfactant (1.8 vol.%)	0.833	1.63	1.36

Determined by Ubbelohde viscosimeter[1] and tensiometer[2]. [3]Containing *N*-isopropylacrylamide (NIPAAm, 98 g L^{-1}), *N*,*N*'-methylenebisacrylamide (BIS, 2 g L^{-1}), ammonium persulfate (APS, 5 g L^{-1}).

As inner phases, either pure water or a pre-microgel fluid were used. The pre-microgel phase for forming pNIPAAm microgels consisted of an aqueous solution of the starting materials *N*-isopropylacrylamide (NIPAAm, 98 $g \cdot L^{-1}$) as monomer and *N*,*N*'-methylenebisacrylamide (BIS, 2 $g \cdot L^{-1}$) as crosslinker, along with a radical initiator, ammonium persulfate (APS, 5 $g \cdot L^{-1}$). After emulsification, this solution can be gelled by free-radical copolymerization.

The formation of droplets was conducted in microfluidic devices with two sequential cross-junctions (Fig. 1B and C). The first junction had a uniform width and height of 40 µm, whereas the second cross-junction had a width of 80 µm along with a constant height of 40 µm. The extra-width at the second junction is added to prevent extensive shear to be imposed on the just-produced droplets, which might potentially split them. With this device, fluid droplets can be formed in the range of ~50 µm in diameter in the first cross-junction and a second fluid can be added in the second junction. Using this setup, the devices were either used in the classical mode of operation with direct surfactant addition in the first, drop-forming cross-junction, as illustrated in Fig. 1B, or alternatively, with delayed surfactant addition at the second junction, as illustrated in Fig. 1C. For simplicity, all microfluidic experiments were performed at equal ratios of flow rates of the inner and outer phases, respectively, $q = q_{\text{aq.phase}} = q_{\text{oil}} = q_{\text{oil+surfactant}}$. The flow rates were all gradually and equally increased to check for when the dripping-to-jetting transition occurs. To discuss this transition in view of the dimensionless Capillary and Weber numbers, Eq. (1) and (2), the viscosities and interfacial tensions of the different fluids were determined (Table 1 and 2). Note that an alternative strategy to approach the jetting-to-dripping transition would be to change the flow-rate ratio of the inner and outer phases rather than fixing it to be equal; however, we refrain from following this approach, as it is equally but not more insightful than operating at fixed flow-rate ratio [10].

Table 2: Mutual interfacial tensions of the fluids used in this work, determined at 25 °C.[1]

	HFE-7500 (mN m^{-1})	HFE-7500 w/surfactant (1.8 vol.%) (mN m^{-1})
Water	15.1	6.09
Monomer solution [2]	1.76	0.60

[1] Determined by tensiometry (Wilhelmy-plate). [2] Containing *N*-isopropylacrylamide (NIPAAm, 98 g L^{-1}), *N*,*N*'-methylenebisacrylamide (BIS, 2 g L^{-1}), and ammonium persulfate (APS, 5 g L^{-1}).

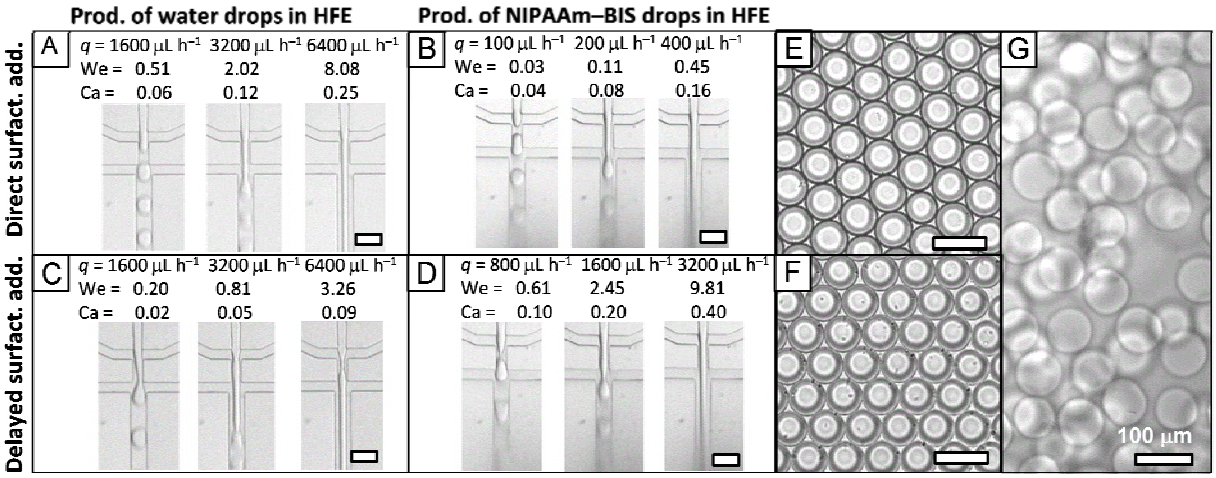

Fig. 2: Dripping-to-jetting transitions in microfluidic emulsification comparing water/HFE oil and NIPAAm/HFE oil systems with either (A, B) direct (first and second cross-junction, each 1.8 vol.%) or (C, D) delayed (only second cross-junction, 3.6 vol.%) surfactant (Krytox 157 FSL) addition. (A, C): Emulsification of water in fluorinated oil HFE-7500. (B, D): Emulsification of an aqueous monomer solution of 98 g L^{-1} NIPAAm, 2 g L^{-1} BIS, and 5 g L^{-1} APS in fluorinated oil HFE-7500. (E), (F): Monodisperse emulsion droplets with droplet diameters of (E) (61 ± 4) µm as obtained in in Panel B at q = 200 µL·h^{-1} and (F) (61 ± 2) µm as obtained in Panel D at q = 1600 µL·h^{-1}. (G) Monodisperse pNIPAAm microgel particles swollen in water as obtained from gelation of the droplets in Panel F. All scalebars denote 100 µm.

The emulsification of pure water in fluorocarbon oil HFE-7500 can be performed at high flow rates with classical direct addition of surfactant in the first microfluidic channel junction (Fig. 2A). The maximum flow rate for controlled dripping was q = 1600 µL·h^{-1}, producing droplets with diameters of 65 ± 2 µm, before jetting was first observed at q = 3200 µL·h^{-1} and then dominated at q = 6400 µL·h^{-1}. These flow rates correspond to Capillary and Weber numbers of $Ca_{,3200}$ = 0.12 and $We_{,3200}$ = 2.02, reflecting the established finding of the dripping-to-jetting transition to occur when either Ca or We or their sum is roughly in the order of unity in a logarithmic dependency [10].

If the inner fluid is more complex and contains a NIPAAm–BIS monomer solution, however, stable and controlled dripping was operable only up to flow rates of q = 100 µL·h^{-1} with direct surfactant addition (Fig. 2B). At higher flow rates, jetting first set in at q = 200 µL·h^{-1} and then dominated at q = 400 µL·h^{-1}, corresponding to $Ca_{,200}$ = 0.08 and $We_{,200}$ = 0.11. This has to be assigned to a tenfold reduction of interfacial tension ($\sigma_{\text{Water / HFE+surfactant}}$ = 6.09 mN·m^{-1}, $\sigma_{\text{NIPAAm–BIS / HFE+surfactant}}$ = 0.6 mN·m^{-1}; Table 2) due to the amphiphilic nature of NIPAAm monomer comprising both hydrophilic and hydrophobic sites.

To overcome the limitation of operating the NIPAAm–BIS emulsification in HFE with controlled dripping only at low flow-rates, we follow the proposed concept of increasing the interfacial tension in the first, drop-forming microfluidic junction by delayed surfactant

addition. In the simple water / HFE system, this approach had not yet a marked effect (Fig. 2C): in this system, the maximum flow rate for controlled dripping was still q = 1600 µL·h^{-1}, again producing droplets with diameters of 63 ± 1 µm at $Ca_{,3200}$ = 0.05 and $We_{,3200}$ = 0.81. By contrast in the NIPAAm–BIS / HFE system, the effect of delayed surfactant addition is notable (Fig. 2D). Here, the onset of jetting did not occur before q = 1600 µL·h^{-1}, corresponding to $Ca_{,1600}$ = 0.20 and $We_{,1600}$ = 2.45, and jetting did not dominate before q = 3200 µL·h^{-1}. Compared to formally q = 200 µL·h^{-1} and q = 400 µL·h^{-1} with direct surfactant addition (Fig. 2B), the delayed surfactant addition increases the volumetric rate of pre-microgel emulsification in the controlled dripping regime by a factor of 8. The size of droplets formed in both of these experimental situations was the same, 61 ± 4 µm for the direct and 61 ± 2µm for the delayed addition of surfactant. As a result, the shown increase of the volumetric rate of droplet formation is also reflected by a strong increase of the number-rate of droplet formation, which is ~500 drops per second in the case of direct surfactant addition compared to ~3800 drops per second in the case of delayed surfactant addition. This marked enlargement in droplet productivity is because of an evident difference in interfacial tension of the NIPAAm–BIS / HFE and the NIPAAm–BIS / HFE+surfactant systems ($\sigma_{\text{NIPAAm–BIS / HFE}}$ = 1.76 mN·m^{-1}, $\sigma_{\text{NIPAAm–BIS / HFE+surfactant}}$ = 0.6 mN·m^{-1}; Table 2). With this improvement, large amounts of nearly monodisperse pre-microgel emulsion droplets with minimal size variation (Fig. 2F) can be prepared in relatively short time.

Subsequent gelation of these droplets was achieved by copolymerization of the monomer and crosslinker within the droplets by their collection in a HFE bath that also contains 1 vol.% of *N*,*N*,*N*',*N*'-tetramethylethylenediamine (TEMED). The latter compound can diffuse into the pre-microgel droplets and catalyze decomposition of the ammonium persulfate radical initiator within them. Thereby, copolymerization of NIPAAm and BIS occurred overnight at room temperature and the droplets gelled, yielding narrowly disperse microgels (Fig. 2G) [6].

Conclusions

Separation of flow-focusing droplet formation and droplet stabilization by delayed addition of surfactant is a simple but efficient strategy to increase the rate of microfluidic-based fabrication of droplets. This strategy can be applied especially to the synthesis of sensitive amphiphilic microgels for applications in various technical and scientific fields including biomedicine. A synergistic combination with existing

approaches like parallelization may push droplet-based microfluidics for microgel-particle fabrication to an industrially relevant scale.

Acknowledgements

Technical support by M. Keller (Institute of Biomaterial Science, Helmholtz-Zentrum Geesthacht) and funding of S. Seiffert by the Berlin Joint Lab for Supramolecular Polymer Systems are acknowledged.

References

[1] W. Funke, O. Okay, B. Joos-Mueller, Adv. Polym. Sci. 136 (1998) 139–234.

[2] A. Pich, H.-J. P. Adler, Polym. Int. 56 (2007) 291–307.

[3] S. Seiffert, Angew. Chem. Int. Ed. 52 (2013) 11462–11468.

[4] H. G. Schild, Prog. Polym. Sci. 17 (1992) 163–249.

[5] J.-W. Kim, A. S. Utada, A. Fernandez-Nieves, Z. Hu, D. A. Weitz, Angew. Chem. Int. Ed. 46 (2007) 1819–1822.

[6] S. Seiffert, ChemPhysChem 14 (2013) 295–304.

[7] D. Velasco, E. Tumarkin, E. Kumacheva, Small 8 (2012) 1633–1642.

[8] S. Xu, Z. Nie, M. Seo, P. Lewis, E. Kumacheva, H. A. Stone, P. Garstecki, D. B. Weibel, I. Gitlin, G. M. Whitesides, Angew. Chem. Int. Ed. 44 (2005) 724–728.

[9] E. Tumarkin, E. Kumacheva, Chem. Soc. Rev. 38 (2009) 2161–2168.

[10] A. S. Utada, A. Fernandey-Nieves, H. A. Stone, D. A. Weitz, Phys. Rev. Lett. 99 (2007) 094502.

[11] T. Nisisako, T. Torii, Lab Chip 8 (2008) 287–293.

[12] T. Nisisako, T. Andoa, T. Hatsuzawa, Lab Chip 12 (2012) 3426–3435.

[13] A. R. Abate, D. A. Weitz, Lab Chip 11 (2011) 1911–1915.

[14] Y. Xia, G. M. Whitesides, Angew. Chem. Int. Ed. 37 (1998) 550–575.

[15] R. K. Shah, J.-W. Kim, J. J. Agresti, D. A. Weitz, L.-Y. Chu, Soft Matter 4 (2008), 2303–2309

[16] Y. Li, T. Tanaka, J. Chem. Phys. 90 (1989) 5161–5166.

[17] C. Holtze, A. C. Rowat, J. J. Agresti, J. B. Hutchison, F. E. Angilè, C. H. J. Schmitz, S. Koester, H. Duan, K. J. Humphry, R. A. Scanga, J. S. Johnson, D. Pisignano and D. A. Weitz, Lab Chip 8 (2008) 1632–1639.